Published in : Colloids and Surfaces B: Biointerfaces (2024), vol. 235, 113788
DOI: 10.1016/j.colsurfb.2024.113788
Status : Postprint (Author's version)

DIVERSELY SUBSTITUTED POLY(N-VINYL AMIDE) DERIVATIVES TOWARDS NON-TOXIC, STEALTH AND PH-RESPONSIVE LIPID NANOCAPSULES

François Toussaint[a], Elise Lepeltier [b,c], Florence Franconi[b], Vincent Pautu[b], Christine Jérôme **a**, Catherine Passirani [b,*], Antoine Debuigne [a,*]

a Center for Education and Research on Macromolecules (CERM), Complex and Entangled Systems from Atoms to Materials Research Unit (CESAM), University of Liàge (ULiège), 4000 Liège, Belgium
b Micro et Nanomédecines Translationnelles (MINT), University of Angers, INSERM 1066, CNRS 6021, Angers, France
c Institut Universitaire de France (IUF), France
** Corresponding authors. E-mail addresses: catherine.passirani@univ-angers.fr (C. Passirani), adebuigne@uliege.be (A. Debuigne).*

KEYWORDS

Lipid nanocapsules - Drug delivery - Stealth properties - pH-responsive nanocarrier - Poly(vinyl pyrrolidone) - Poly(N-methyl-N-vinyl acetamide)

ABSTRACT

Surface modification of lipid nanocapsules (LNC) is necessary to impart stealth properties to these drug carriers and enhance their accumulation into the tumor microenvironment. While pegylation is commonly used to prolong the circulation time of LNC, the increased presence of anti-PEG antibodies in the human population and the internalization issues associated to the PEG shell are strong incentives to search alternatives. This work describes the development of amphiphilic poly(N-vinyl amide)-based (co)polymers, including pH-responsive ones, and their use as LNC modifiers towards improved drug delivery systems. RAFT polymerization gave access to a series of LNC modifiers composed of poly(*N*-methyl-*N*-vinyl acetamide), poly(*N*-vinyl pyrrolidone) or pH-responsive vinylimidazole-based sequence bearing a variety of lipophilic end-groups, namely octadecyl, dioctadecyl or phospholipid groups, for anchoring to the LNC. Decoration of the LNC with these families of poly (N-vinyl amide) derivatives was achieved via both post-insertion and per-formulation methods. This offered valuable and non-toxic LNC protection from opsonization by complement activation, emphasized the benefit of dioctadecyl in the per-formulation approach and highlighted the great potential of poly(*N*-methyl-*N*-vinyl acetamide) as PEG alternative. Moreover, incorporation of imidazole moieties in the shell of the carrier imparted pH-responsiveness to the LNC likely to increase the cellular uptake in the acidic tumor microenvironment, opening up new possibilities in the field of active targeting.

Published in : Colloids and Surfaces B: Biointerfaces (2024), vol. 235, 113788
DOI: 10.1016/j.colsurfb.2024.113788
Status : Postprint (Author's version)

Introduction

The last decades have witnessed great progress in nanomedicines and implementation of effective targeted therapies especially in oncology [1–3]. In general, encapsulation of drugs in nanocarriers provides several medical and pharmaceutical benefits such as control of the solubility, the vascular circulation time enhancement and the specific site-targeted delivery of the drug. Passive and/or active targeting of the tumor cells and tissues by the anticancer-loaded carriers allows to reduce the amount of administrated drug and to preserve the healthy cells. Among the wide variety of drug nano-vectors such as liposomes, nanoparticles, micelles or polymer-drug conjugates, the lipid nanocapsules (LNC) are particularly attractive [4]. These nano-cargos, manufactured by a phase inversion temperature (PIT) process [5], are characterized by a diameter ranging from 20 to 100 nm according to their composition. LNCs are composed of an oily core of triglycerides surrounded by a tensioactive membrane of polyethylene glycol (PEG). Compared to other carriers including liposomes, they exhibit a higher stability in biological fluids and allows a high loading of diverse lipophilic drugs. For example, paclitaxel-loaded LNC improved the anticancer hydrophobic drug bioavailability while overcoming multidrug resistance (MDR) for rat glioma [6]. Some etoposide-containing LNCs demonstrated ability to suppress glioma cell growth by intracellular drug delivery and simultaneous P-glycoprotein inhibition [7]. Curcumin-loaded LNC allowed to bypass the P-glycoprotein mediated doxorubicin resistance in triple negative breast cancer cells [8]. Other studies validated the efficacy of ferrocifen-loaded LNC against MDR tumors, in particular in malignant glioma models [9–17].

For these applications, modification of the LNC surface with polymers was necessary to impart them stealth properties and to allow their accumulation into the tumor microenvironment via the Enhanced Permeation and Retention (EPR) effect [18,19]. Owing to the elasticity of the LNC shell [20], the latter was easily modified by post-insertion of PEGylated phospholipid, namely 1,2-distearoyl-sn-glycero-3-phosphoe- thanolamine-N-[amino(polyethylene glycol)-2000] (DSPE-PEG2000) [18,19]. Given the increased presence of anti-PEG antibodies in the general human population [21], however, the search for PEG alternative remains topical [22,23]. Two polysaccharides were notably post-inserted into the LNC shell, namely lipodextran and a positively charged lipochitosan [24]. Such modifications neither enhanced nor deteriorated the carrier biodistribution and pharmacokinetics and the chitosan-modified LNC paved the way to functionalization by negatively charged and active molecules like siRNA or peptides. Active targeting strategies, involving peripherally conjugated targeting moieties such as aptamers, antibodies or cell-penetrating peptides, have also been implemented to improve the selective LNC accumulation and delivery in the diseased tissues. For

Published in : Colloids and Surfaces B: Biointerfaces (2024), vol. 235, 113788
DOI: 10.1016/j.colsurfb.2024.113788
Status : Postprint (Author's version)

example, an antibody Fab' fragment was covalently grafted via thiol-maleimide conjugation onto DSPE-PEG2000-maleimide functional LNC [25]. Moreover, surface-functionalization of LNC with the cell-penetrating peptides NFL-TBS-40–63 was achieved by adsorption and enhanced the nanocarrier internalization into human glioblastoma cells [26]. Some stimuli responsive LNCs were also designed to promote the specific drug delivery in the tumor under intrinsic physicochemical and pathological factors. In a recent preliminary work, stearyl-functionalized *N*-vinyl pyrrolidone/vinyl imidazole-based copolymers were post-inserted onto LNC instead of the DSPE-PEG [27]. This modification not only protected the nanocarrier from opsonization by the complement activation but also favored its cellular uptake and biological effect via protonation of the imidazole moieties of the shell due to the pH decrease in the tumoral vicinity [27]. On the other hand, recent studies demonstrated that modifying liposomes and lipid nanoparticles (LNPs) with PNMVA instead of PEG or poly(*N*-vinyl pyrrolidone) (PNVP) had a positive effect on both immunogenicity and siRNA transfection efficiency of the carriers [28,29].

This work reports on the surface modification of LNC by a library of novel amphiphilic poly(N-vinyl amide) derivatives towards non-toxic, stealth and pH-responsive nanocarriers for improved drug delivery system (Fig. 1). Besides the well-known biocompatible PNVP, PNMVA with acyclic amide pendent functions was considered as hydrophilic sequence for the modification of LNCs for the first time. Moreover, various hydrophobic groups such as octadecyl, dioctadecyl as well as DSPE, were considered in order to tune the anchoring capacity of the later at the surface of the LNCs. Bearing in mind that the appearance of charges at the surface of the nanocarriers in the vicinity of the tumoral cells enhances their internalization [27], the incorporation of 1-vinyl imidazole in the copolymer shell and pH-responsiveness of the corresponding LNC was also examined. Polymer syntheses were performed by reversible addition fragmentation chain transfer (RAFT) [30–32], a reversible deactivation radical polymerization (RDRP) technique suitable for less activated monomers [33,34] such as NVP [35–38] and NMVA [39], in order to control the molar mass of the hydrophilic segment and guarantee its proper functionalization by the hydrophobic group. In addition to the traditional LNC post-modification method, lipid nanocapsules were also formulated directly in the presence of poly (N-vinyl amide)-based (co)polymers. The influence of all these parameters, namely copolymer structure varying both the lipophilic and hydrophilic sequences, pH change, post-insertion versus per-formulation methods, on the physicochemical characteristics, stealth properties and in vitro cell toxicity (on B16F10 and HepG2) of the accordingly functionalized LNC was evaluated.

Published in : Colloids and Surfaces B: Biointerfaces (2024), vol. 235, 113788
DOI: 10.1016/j.colsurfb.2024.113788
Status : Postprint (Author's version)

Materials and methods

MATERIALS

Caprylic-capric acid triglycerides (Labrafac WL 1349®, Gatefossé S. A., France), hydroxystearate-PEG (Kolliphor® HS 15, BASF, Germany), NaCl (VWR) and lecithin (Lipoid S100®, Lipoid GmbH, Germany) were used as received for the preparation of the LNC. Sodium phosphate buffer solutions at different pH (7.4, 6.8, 6.5, 6) were prepared from sodium phosphate monobasic monohydrate and sodium phosphate dibasic heptahydrate to reach a final concentration in phosphate of 1 mM in miliQ water.

SYNTHESIS OF THE POLY(N-VINYL AMIDE)S DERIVATIVES

Fig. 1. *Surface decoration of LNCs with amphiphilic poly(N-vinyl amide) derivatives by per-formulation or post-modification methods.*

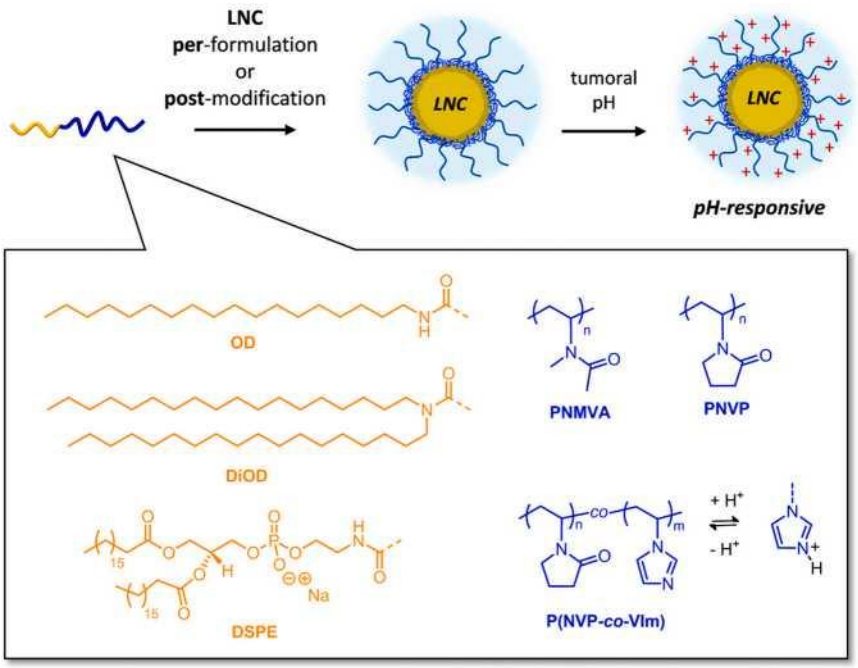

Synthesis and characterization of the poly(N-vinyl amide)s derivatives and of their precursors are inspired from references [28,29] and described in details in the supporting information section.

Published in : Colloids and Surfaces B: Biointerfaces (2024), vol. 235, 113788
DOI: 10.1016/j.colsurfb.2024.113788
Status : Postprint (Author's version)

BLANK LNC (BLK) FORMULATION

Lipid nanocapsules were formulated by a phase inversion temperature process, as previously described [5,40,41]. Briefly, 20.2 % w/w caprylic-capric acid triglycerides, 17.2 % w/w hydroxystearate-PEG, 1.8 % w/w NaCl, 1.5 % w/w lecithin and 35.58 % w/w of milliQ water were mixed under magnetic stirring. Three cycles of heating and cooling between 60 and 90 °C were carried out to obtain the phase inversion from an o/w emulsion to a w/o emulsion. Ice cooled milliQ water 23.72 % w/w was added at the last phase inversion zone (PIZ) leading to the formation of lipid nanocapsules.

POLYMER POST-INSERTION

LNC and polymers were mixed in miliQ water and co-incubated for 2 h at 60 °C under magnetic stirring with a final polymer concentration of 0.5 mM or 1 mM. The mixture was then cooled down for 20 min in an ice bath, under magnetic stirring. As control, to obtain unmodified LNC (BLK LNC C), the same protocol was applied using the same dilution factor without adding the polymer (two controls per post-modification). After post-insertion, decorated LNC were filtrated through 0.22 µm filter.

LNC PER-FORMULATION

Lipid nanocapsules per-formulated with polymers were synthesised similarly to the BLK formulations. Briefly, 20.2 % w/w caprylic-capric acid triglycerides, 17.2 % w/w hydroxystearate-PEG, 1.8 % w/w NaCl, 1.5 % w/w lecithin, 35.58 % w/w of milliQ water and polymer (1 mM in the final volume) were mixed under magnetic stirring. Three cycles of heating and cooling between 60 and 90 °C were carried out to obtain the phase inversion. Ice cooled milliQ water 23.72 % w/w was added at the last inversion temperature leading to the formation of lipid nanocapsules.

SIZE AND ZETA POTENTIAL MEASUREMENTS

The mean diameter in intensity and polydispersity index (PDI) of LNC were measured using the Dynamic Light Scattering (DLS) method at a backscatter angle of 173°. Zeta potential was measured using the laser Doppler micro-electrophoresis technique with a Malvern Zetasizer® apparatus (Nano Series ZS, Malvern Instruments S.A., UK) at 25 °C. Measurements were performed by diluting LNC 10 times in 1 mM phosphate buffer NaH_2PO_4/Na_2HPO_4 at different pH: 7.4, 6.8, 6.5, 6. Experiments were conducted 3 times with a measured average value calculated from 3 runs, with 12 measurements by run for size and 20 measurements by run for

Published in : Colloids and Surfaces B: Biointerfaces (2024), vol. 235, 113788
DOI: 10.1016/j.colsurfb.2024.113788
Status : Postprint (Author's version)

zeta potential.

STABILITY STUDY

LNC were kept at 4 °C. Stability in size, PDI and zeta potential was evaluated over 14 days. Experiments were performed using the method described above.

BUFFERING EFFECT

The buffering capacities of the different polymers alone and post-inserted into LNC were measured by acid base titration according to the method described by Zhong *et al* [42]. Polymers were solubilized in 0.1 M aqueous NaCl to reach a concentration of 0.1 mM. 10 mL of the 0.1 mM polymer solutions were adjusted initially to pH 11 with 0.1 M NaOH. Then, the solutions were titrated to reach pH 3 by adding 0.1 M HCl. After each addition of 25 µL of HCl, pH was measured with a pH

meter. Endosome buffering capacity was evaluated as the amount of HCl to modify the solution pH from 7.4 to 5.1.

CELL CULTURE

The B16F10 mice melanoma cell line (gift from University of Brussels) was grown in Roswell Park Memorial Institute (RPMI) 1640 medium (Lonza, Verviers, Belgium) supplemented with 10 % heat- inactivated FBS (Lonza), 1 % antibiotic and antimycotic solution (Sigma-Aldrich) and 1 % non-essential amino acids (Lonza). Cell lines were cultured and maintained at 37 °C in a humidified atmosphere with 5 % CO_2. The HepG2 cell line, obtained from ATCC (HB-8065), was grown in minimum essential media (MEM) (Gibco, Thermofisher) supplemented with 10 % heat-inactivated FBS (Lonza), 1 % antibiotic and antimycotic solution (Sigma-Aldrich) and 1 % non-essential amino acids (Lonza).

MTT CELL VIABILITY ASSAY

B16F10 and HepG2 cells were cultured in a 96 well plate at a density of 5.10^3 cells/well and 2.10^4 cells/well respectively, and incubated for 24 h. Cells were then treated for 24 h with 100 µL/well of media containing either post-inserted LNCs at a concentration range of 10 µg/mL to 1000 µg/mL or polymers at the concentration corresponding to the LNC dilutions (0.025 µM to 2.5 µM). Cytotoxicity was determined with a colorimetric assay, using the succinate dehydrogenase activity of viable cells via the reduction of the yellow-

Published in : Colloids and Surfaces B: Biointerfaces (2024), vol. 235, 113788
DOI: 10.1016/j.colsurfb.2024.113788
Status : Postprint (Author's version)

colored tetrazolium salt, 3-(4,5- dimethylth-iazol-2-yl)-2,5-diphenyl tetrazolium bromide to a purple-colored formazan crystal (MTT assay - Sigma-Aldrich, France). Concretely, 10 µL of MTT (5 mg/mL) was added to each well and the plates were incubated for 4 h under a humidified atmosphere with 5 % CO2. The media was then aspirated and the formazan crystals were solubilized with 100 µL of dimethyl sulfoxide (DMSO - Sigma-Aldrich, France). The absorbance was then measured at 560 nm wavelength using a Spectra Max M2™ Microplate reader (Molecular Devices, France). Experiments were repeated three times with three replicates per experiment.

COMPLEMENT ACTIVATION

Complement activation was determined by measuring the lytic capacity of normal human serum after exposure to the LNC according to Passirani *et al* [43]. Briefly, normal human serum (NHS) (provided by the Etablissement Français du Sang (Angers, France)) was diluted in veronal-buffered saline containing 0.15 mM Ca^{2+} and 0.5 mM Mg^{2+} (VBS^{++}) and incubated for 1 h at 37 °C with an increased concentration of LNCs. The suspension was then diluted in VBS^{++} (1/25 v/v) and incubated for 45 min at 37 °C with sheep erythrocytes (Labor Dr. Merk, Germany) sensitized by rabbit anti-sheep erythrocyte antibodies (Eurobio, France). The suspension was centrifuged at 800 g for 10 min. Light absorption of supernatant was then read at 405 nm with a microplate reader (Multiskan Ascent, Labsystems SA, France).

The amount of serum able to lyse 50 % of sensitized erythrocytes (CH50) was calculated for each sample using the following formula:

$$consumption \quad (\%) = \frac{\left(CH50_{sample} - CH50_{control}\right) \times 100}{CH50_{control}}$$

To compare the different modified LNCs, the complement consumption was plotted as a function of the surface area. Surface area was calculated using formula described previously [43].

Results and discussion

SYNTHESIS OF POLY(N-VINYL AMIDE)-BASED LNC MODIFIERS

A series of innovative LNC modifiers was prepared by functionalizing a hydrosoluble poly(N-vinyl amide) sequence, namely PNVP or PNMVA, with different hydrophobic groups such as octadecyl (OD), dioctadecyl

Published in : Colloids and Surfaces B: Biointerfaces (2024), vol. 235, 113788
DOI: 10.1016/j.colsurfb.2024.113788
Status : Postprint (Author's version)

(DiOD) and 1,2-distearoyl-sn-glycero-3-phosphoethanolamine (DSPE). The general synthesis strategy, inspired from recent reports on the design of poly(N-vinyl amide)-based derivatives for the modification of lipoplexes [28,29], relies on the RAFT polymerization using xanthate as chain transfer agent (CTA) (Fig. 2). For the sake of the application, degree of polymerizations (DPs) ranging from 30 to 50 were targeted. The macromolecular characteristics of the poly(N-vinyl amide)-based (co) polymers made available for the surface modification of LNCs are summarized in the table inset of Fig. 2 and polymerization conditions are commented below.

First, the RAFT polymerization of NVP was carried out at 60 °C in the presence of a xanthate containing an octadecyl group in its initiating fragment (OD-XA) and of 20 mol% of AIBN compared to the CTA (Fig. 2 route A, Table S1 entries 1 and 2). NVP/OD-XA molar ratios of 50 and 100 were considered leading to amphiphilic OD-PNVP derivatives of low dispersity ($Đ$ ~ 1.2–1.3) and DP of 31 and 46, respectively (**P1** and **P2** in Fig. 2, Table S1 entries 1 and 2). Similarly, a DiOD-PNVP characterized by a DP of 44 was produced using a dioctadecyl-containing RAFT CTA (**P3** Fig. 2, Table S1 entry 3). As reported [28], proper NVP polymerization required 50 mol% of AIBN compared to the DiOD-XA and a slightly higher temperature (65 °C) probably to ensure proper solubility of the double aliphatic chain of the CTA. Finally, the synthesis of DSPE-PNVP **P4** was achieved via RAFT of NVP at 60 °C involving a succinimidyl carbonate xanthate (SC-XA) (Table S1 entry 4) followed by quantitative coupling of the amino group of DSPE and the terminal succinimidyl carbonate of PNVP at 40 °C (Fig. 2 route B, Table S1 entry 5). Structures of these functional PNVPs were confirmed by ^{1}H NMR (Fig. S1). Besides typical signals of PNVP, characteristic peaks of the different hydrophobic groups (OD-, DiOD-, DSPE-) were clearly identified. It is noteworthy that the intensity of ^{1}H signal corresponding to the terminal xanthate (-SC(S)CH_2CH$_3$ at 4.6 ppm) is very weak compared to the methyl signal of the hydrophobic group in alpha position of the chain (at 0.8 ppm), suggesting the removal of the xanthate during the purification process via prolonged dialysis in water, in agreement with degradation reactions described by Pound *et al* [38].

Recently, Destarac *et al.* reported the first synthesis of well-defined PNMVA via xanthate-mediated radical polymerization at low temperature using V70 as radical initiator [39]. Inspired by this pioneering work, we adapted the above mentioned procedure and prepared the corresponding OD-PNMVA31 (**P5**) and DSPE-PNMVA44 (**P6)** via RAFT polymerization of NMVA at 30 °C using OD-XA and SC-XA as CTAs, respectively (Fig. 2 routes A and B, Table S1 entries 6–8). Eventually, the ^{1}H NMR allowed to confirm the structure and to determine the DP of OD-PNMVA31 and DSPE-PNMVA44 (Fig. S2).

In order to impart pH-responsiveness to the poly(N-vinyl amide) derivatives, we considered the incorporation

Published in : Colloids and Surfaces B: Biointerfaces (2024), vol. 235, 113788
DOI: 10.1016/j.colsurfb.2024.113788
Status : Postprint (Author's version)

of imidazole moieties along their polymer backbone via copolymerization of VIm (Fig. 2 route C). Considering the previous successful xanthate-mediated radical homopolymerization of VIm in DMF [44,45], the RAFT copolymerization of NVP/VIm was performed in DMF using xanthate functionalized by an ethyl group (Et-XA) as model reaction (Fig. 2, Table S2). The NVP/VIm copolymerization occurred at 65 °C but the conversion remained quite limited after 24 h (Table S2 entry 1). Increasing the polymerization temperature to 80 °C improved the conversion, leading to a NVP/VIm copolymer with moderate dispersity and molar mass in the targeted range (Table S2 entry 2). Finally, conversion further increased when using 50 mol% of AIBN instead of 20 mol% but polymers with much broader dispersity were obtained accordingly (Table S2 entry 3). On this basis, 80 °C in DMF using 20 mol% of AIBN compared to the RAFT agent appeared as best conditions. As illustrated by Fig. S3, the copolymer compositions were measured by ^{1}H NMR and revealed the incorporation of about 39–43 mol% of VIm when starting from a molar fraction of VIm of 0.3 in the feed, suggesting the preferential incorporation of VIm over NVP during the copolymerization.

These optimized conditions, namely 80 °C in DMF with 0.2 equivalent of AIBN, were applied to the RAFT copolymerization of NVP/VIm using OD-XA as CTA (Fig. 2 route C, Table S3 entry 1). After 24 h, an OD- P(NVP-co-VIm) (**P7**) with a dispersity of about 1.6 and composed of 43 mol% of VIm according to the ^{1}H NMR (Fig. S4) was collected. In contrast, no polymer was produced with DiOD-XA under these conditions (Table S3 entry 2). Increasing the AIBN content to 0.5 equivalent compared to the CTA, however, gave access to the targeted DiOD-P (NVP-co-VIm) with different molar masses depending on the monomer/DiOD-XA ratio (Table S3 entries 3 and 4, **P8**). ^{1}H NMR spectra of OD-P(NVP-co-VIm) (**P7**) and DiOD-P(NVP-co-VIm) (**P8**) are provided in Fig. S4. The composition of these NVP/VIm copolymers (F_{VIm} ~0.40–0.45) was determined by comparing the intensity of the aromatic protons (**m**-**o**) from the imidazole ring between 6.75 and 7.90 ppm and the cumulated intensity of peaks between 2.76–4.30 ppm assigned to protons **g** and **h** of NVP units and methyne proton **l** of VIm units.

Published in : Colloids and Surfaces B: Biointerfaces (2024), vol. 235, 113788
DOI: 10.1016/j.colsurfb.2024.113788
Status : Postprint (Author's version)

Fig. 2. *Synthesis and characteristics of the NVP- and NMVA-based (co)polymers used as LNC modifiers. DP and M_n (number average molecular weight) were determined by ^{1}H NMR.*

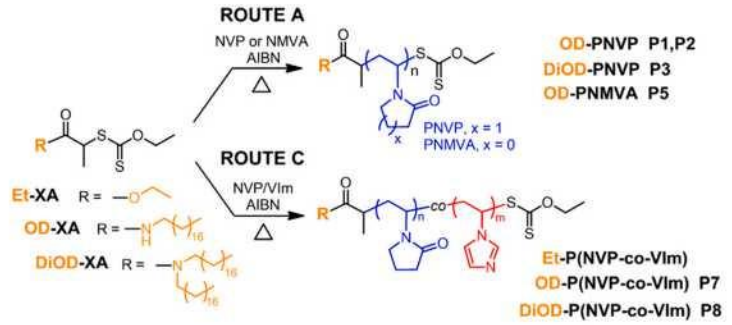

	Polymer	DP	M_n (g.mol^{-1})
P1	OD-PNVP$_{31}$	31	3400
P2	OD-PNVP$_{46}$	46	5100
P3	DiOD-PNVP$_{44}$	44	4900
P4	DSPE-PNVP$_{47}$	47	5200
P5	OD-PNMVA$_{31}$	31	3100
P6	DSPE-PNMVA$_{44}$	44	4400
P7	OD-P(NVP$_{27}$coVIm$_{21}$)	48	5000
P8	DiOD-P(NVP$_{22}$coVIm$_{15}$)	37	3900

Because the position of the imidazole group along the poly(N-vinyl amide) chain is likely to influence the final properties of the modified LNC, we determined the NVP/VIm reactivity ratios in order to gain insight into the comonomer distribution. For this purpose, a series of RAFT co-polymerizations of NVP/VIm were initiated by OD-XA, at 80 °C in DMF, with various comonomers molar feed ratios (*f*). Each experiment was stopped at low conversion and the final composition was determined by ^{1}H NMR (Table S4). Based on these data, reactivity ratios were determined by the non-linear least squares method[46,47] based on the Mayo–Lewis equation (Fig. S5A) as well as the Finemann–Ross[48] (Fig. S5B) and Kelen-Tüdös[49] (Fig. S5C) methods. Values determined by these different methods were fully consistent with correlation factors of 0.99. Reactivity ratios around r_{NVP} = 0.55 and r_{VIm} = 1.20 were obtained suggesting a preferential incorporation of VIm in the copolymer. Based on the Skeist's model (SK) and the reactivity ratios determined beforehand, Fig. S6 predicts the evolution of the instantaneous feed and copolymer compositions (f_{inst} and $F_{inst,}$ respectively) as well as the cumulative copolymer composition (F_{cumul}) as a function of the overall conversion when starting from a comonomer feed containing 30 mol% of VIm. In this case, only a slight composition drift (a few percent below 70 % of total monomer conversion) was observed, suggesting a relatively homogeneous distribution of the VIm units along the P (NVP-co-VIm) copolymer chain.

Finally, although SC-P(NVP-co-VIm) could be produced under similar conditions, attempts to couple the latter with DSPE remained unsuccessful. Moreover, efforts to copolymerize VIm with NMVA did not succeed due to

Published in : Colloids and Surfaces B: Biointerfaces (2024), vol. 235, 113788
DOI: 10.1016/j.colsurfb.2024.113788
Status : Postprint (Author's version)

the important gap between the ideal RAFT temperatures for VIm and NMVA, namely 80 °C and 30 °C, respectively. After all, the diversely substituted poly(N-vinyl amide)s (**P1**-**P8**) synthesized in this section were tested for the surface decoration of LNCs.

LNC SURFACE FUNCTIONALIZATION

Lipid nanocapsules, composed of caprylic-capric acid triglycerides, were formulated via a classical phase inversion temperature (PIT) process described by Heurtault *et al* [5]. These blank LNCs were characterized by a mean diameter of about 55 nm, a low polydispersity index (0.02–0.03) and a slightly negative Zeta-potential in agreement with previous characterization of blank LNCs [50]. These LNCs were then post-inserted at 60 °C by the poly(N-vinyl amide) derivatives (P1-P8) depicted in Fig. 2. A group control (Blank LNC C) was also produced by applying the same thermal treatment to LNCs in absence of polymer.

Mean diameter, polydispersity index and Zeta-potential of LNCs post-modified by the different polymers (P1-P8) at a concentration of 1 mM are presented in Fig. 3. Fig. S7 depicts representative DLS plots for various LNC formulations, illustrating a consistent monomodal distribution in all cases. For LNCs decorated with PNVP-based derivatives (LNC P1-LNC P4), an increase of around 5 nm in diameter was observed compared to the reference samples, suggesting the successful modification of the lipid nanocapsules. Logically, this increase was more limited when the DP of PNVP was low (compare LNC P1 and LNC P2 modified with OD-$PNVP_{31}$ and OD-$PNVP_{46}$, respectively). In accordance with the neutral character of PNVP, post-modification of LNCs with such derivatives did not alter the surface charge of the carrier, except for LNC P4. The latter exhibited a negative charge surface of about -10 mV that was attributed to the phosphate group of DSPE. Very similar trends were observed when substituting PNVP for PNMVA, namely limited size increase of the LNCs modified by OD-$PNMVA_{31}$ (LNC P5) and DSPE- $PNMVA_{44}$ (LNC P6) as well as appearance of a negative charge at the surface of LNC P6. The effect of pH on the characteristics of all these post-modified LNCs was negligible. The same cannot be said for the LNCs treated with NVP/VIm-based copolymers (P7 and P8). In these cases, the increase in diameter and polydispersity index was more pronounced (mean diameter up to 70 nm and polydispersity index around 0.08) suggesting a successful modification of the LNCs. Moreover, the surface charge of LNC P7 and LNC P8 was slightly positive at neutral pH and regularly increased to about + 12 mV when decreasing the pH to 6 as a result of the protonation of the pendant imidazole moieties. This observation is consistent with the literature describing VIm-based polymers with pKa around 6–7 [51,52]. Overall, protonation of the imidazole group of the LNC shell of LNC P7 and LNC P8 should occur in an extracellular

Published in : Colloids and Surfaces B: Biointerfaces (2024), vol. 235, 113788
DOI: 10.1016/j.colsurfb.2024.113788
Status : Postprint (Author's version)

tumor pH of 6.5 or below [53] triggering the appearance of a positive charge at the surface of the LNCs and, ultimately, improving their cell internalization [27]. As depicted by Fig. S8, the modified LNCs (LNC P1-LNC P8) exhibited good stability after 2 weeks.

In order to limit the amount of polymers involved in the modification of LNCs and to probe the possible differences in the polymer anchoring as a function of its hydrophobic group, post-insertions of P7 and P8 within the LNCs were implemented at lower concentration, namely 0.5 mM instead of 1 mM (see LNC P7′ and LNC P8′ in Fig. 4). The decrease in polymer concentration did not affect the final characteristics of the LNCs exhibiting similar size, polydispersity index and pH responsiveness. No major difference was also observed between LNC P7′ and LNC P8′ suggesting that, under these conditions, a simple OD chain is as effective anchoring group as DiOD which mimics the double aliphatic chains of phospholipids.

At this stage, all surface modifications of LNCs were accomplished via a post-insertion procedure but the one-step per-formulation method, in which the LNCs are formulated in the presence of the polymer modifier, remains appealing and was tested (Fig. 4). For the LNCs produced in the presence of the OD-P(NVP$_{27}$-*co*-VIm$_{21}$) (LNC P7 *), no significant difference was observed compared to its post-modified counterpart (LNC P7), except maybe a lower positive charge surface upon pH decrease.

Fig. 3. *Physicochemical characterization of blank LNC (BLK LNC) and LNC post-inserted by OD-PNVP31 (P1), OD-PNVP46 (P2), DiOD-PNVP44 (P3), DSPE-PNVP47 (P4), OD-PNMVA$_{31}$ (P5), DSPE-PNMVA$_{44}$ (P6), OD-P(NVP$_{27}$-co-VIm$_{21}$) (P7) and DiOD-P(NVP$_{22}$-co-VIm$_{15}$) (P8): hydrodynamic diameter determined with mean intensity (nm) (A), polydispersity index (PDI) (B) and Zeta potential (mV) (C) at different pH: 7.4, 6.8, 6.5 and 6. Results (n = 3) are expressed as mean measure ± SEM.*

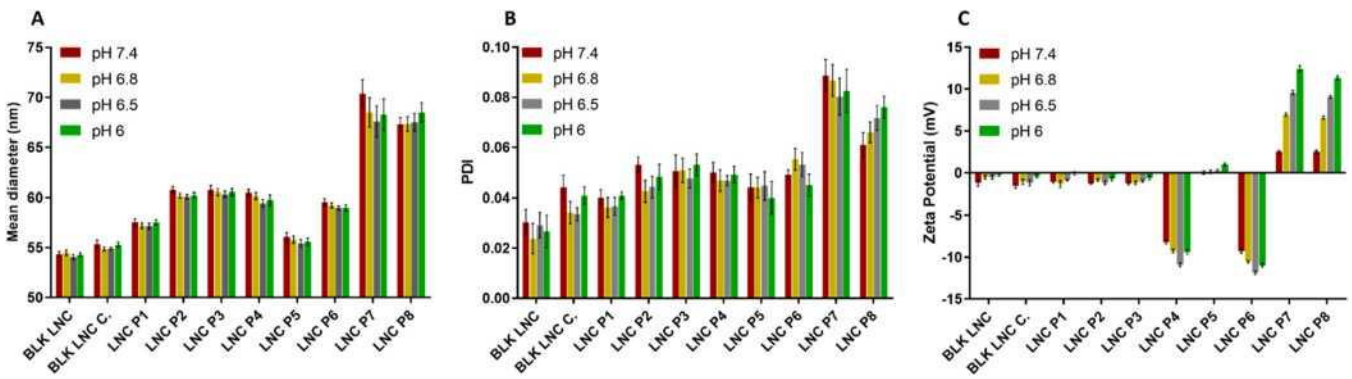

Published in : Colloids and Surfaces B: Biointerfaces (2024), vol. 235, 113788
DOI: 10.1016/j.colsurfb.2024.113788
Status : Postprint (Author's version)

Fig. 4. *Physicochemical characterization of blank LNCs and LNCs modified by P7 (OD-P(NVP$_{27}$coVIm$_{21}$)) and P8 (DiOD-P(NVP$_{22}$coVIm$_{15}$)). LNCs post-inserted with 1 mM of P7 (LNC P7) or P8 (LNC P8); LNCs post-inserted with 0.5 mM of P7 (LNC P7') or P8 (LNC P8'); LNCs per-formulated with 1 mM of P7 (LNC P7 *) or P8 (LNC P8 *): hydrodynamic diameter determined with mean intensity (nm) (A), polydispersity index (PDI) (B) and Zeta potential (mV) (C) at different pH: 7.4, 6.8, 6.5 and 6. Results (n = 3 for BLK, LNC P7 and LNC P8; n = 1 for LNC P7' and LNC P8', n = 2 for LNC P7 * and LNC P8 *) are expressed as mean measure ± SEM.*

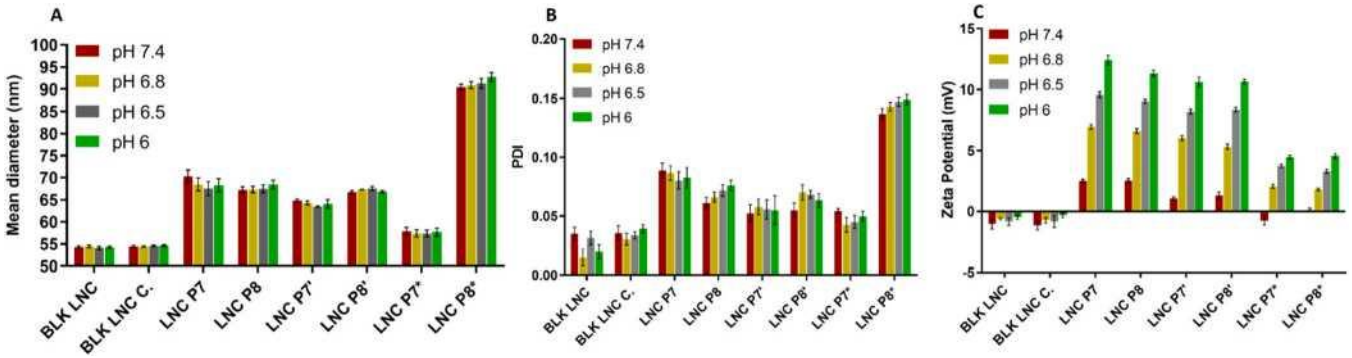

This might be due to partial encapsulation of P7 within the core of the LNCs. For P8, however, the diameter and polydispersity index of the pre-inserted LNC (LNC P8 *) was found much higher compared to LNC P8 indicating the greater impact of the DiOD group on the LNC formation process compared to OD. Again, the Zeta-potential of LNC P8 * did not exceed + 5 mV at pH 6 indicating a lower amount of the pH-responsive polymer at the LNC surface. Although moderate, this positive charge should be sufficient to promote interactions of the LNCs with cell membranes and to enhance the cellular uptake.

BUFFERING EFFECT

The different LNC modifiers were then subjected to acid-base titration in order to assess their ability to promote endosomal escape via buffering effect (Fig. 5). In practice, the buffering capacity of the polymers relates to the HCl amount needed to promote a pH decrease from 7.4 to 5.1. Fig. 5 clearly shows a rapid pH drop upon HCl addition to aqueous solutions of PNVP- and PNMVA-based derivatives (P1-P4 and P5-P6, respectively), confirming the absence of buffering effect, consistently with the lack of protonable group in their structure. In contrast, for the VIm-containing LNC modifiers (P7 and P8), the addition of HCl decreased the pH value progressively and the slope of the curves changed along the process with a slow decrease in the range of pH 7–3.

Published in : Colloids and Surfaces B: Biointerfaces (2024), vol. 235, 113788
DOI: 10.1016/j.colsurfb.2024.113788
Status : Postprint (Author's version)

Note that the buffering capacity of P7 was greater than that of P8 certainly due to its higher VIm content. As demonstrated for other pH- responsive polymers [51,54,55], the buffering capacities of these P (NVP-co-VIm)-based LNC modifiers is likely to play a major role in the endosomal escape mechanism through the "proton sponge effect".

Fig. 5. *Acid-base titration of polymer (P1-P8) solutions at a concentration 0.1 mM in aqueous NaCl (0.1 M).*

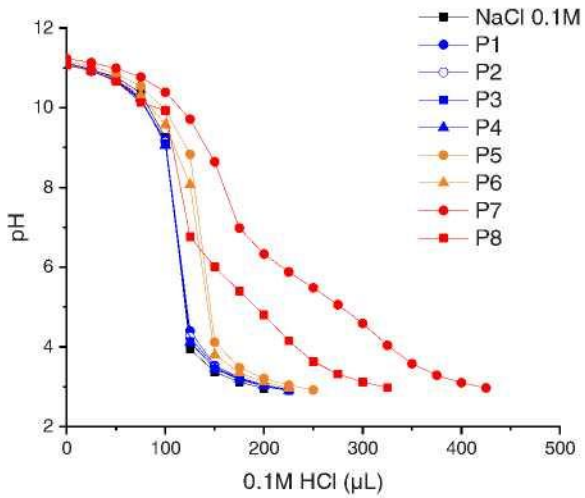

COMPLEMENT ACTIVATION

The complement consumption was analyzed in normal human serum (NHS) by measuring the residual hemolytic capacity of the complement system after contact with the modified LNCs (Fig. 6A). The pH-responsive LNCs (LNC P7 and LNC P8) appeared as the most complement activating carriers. Compared to literature [56], however, the recorded complement activation (CA) levels (20–30 %) remained reasonable until 1500 cm^2/mL and increased to about 50 % in the 2000–3000 cm^2/mL range. In contrast, all PNVP-modified LNCs (LNCs P1-P4) showed complement activation below 20 % even at 3000 cm^2/mL. Indeed, LNC P3 and LNC P4 involving DiOD-PNVP and DSPE-PNVP showed a complement activation level between 10 % and 20 % whereas near-zero complement activation was recorded for LNC P1 and LNC P2 composed of OD-PNVPs. It is noteworthy that the PNMVA-modified LNCs (LNC P5 and LNC P6) showed no tendency to activate the complement whatever the hydrophobic group (OD or DSPE) associated to PNMVA. This demonstrates that the use of PNMVA for decorating LNCs ensures their stealth properties. Moreover, the stealth behavior of these PNMVA-modified nanocarriers should persist after repeated injection as suggested by a recent study[29]

Published in : Colloids and Surfaces B: Biointerfaces (2024), vol. 235, 113788
DOI: 10.1016/j.colsurfb.2024.113788
Status : Postprint (Author's version)

revealing that PNMVA does not induce an accelerated blood clearance (ABC) effect in contrast to PEG. Interestingly, the complement activation propensity of the VIm-containing LNCs could be lowered by decreasing the amount of polymer involved in the post-modification of LNCs (0.5 mM, LNCs P7′ and P8′) (Fig. 6B) while preserving in large part their pH response (Fig. 4C). Furthermore, moving from post-insertion to per-formulation of P7 in the LNC (LNC P7*) did not modify the way it activates the complement. However, when considering per-formulation of P8 (LNC P8*), the complement activation reached its lowest level while keeping a similar pH-response compared to LNC P7* (Fig. 4C). The explanation for the complement activation difference observed between the per-formulated LNC P8* and the post-modified LNC P8 is not straight-forward. Indeed, the low opsonization of per-formulated P8* appears to be the result of a lower functionalization density with P(NVP-co-VIm) suggested by the lower charge surface of the LNC (compare LNC P8 and LNC P8* in Fig. 4C). Although it would have been interesting to assess the quantity of polymer present on the surface of both LNCs, our efforts in this regard, notably through DOESY NMR, remained unsuccessful. The challenge relies on the minimal polymer concentration and its distribution among the solution, surface, and core of the particle.

Fig. 6. *Complement consumption at 37 °C of (A) blank LNCs (BLK LNC) and LNCS post-inserted at 1 mM with OD-PNVP$_{31}$ (LNC P1), OD-PNVP$_{46}$ (LNC P2), DiOD- PNVP$_{44}$(LNC P3), DSPE-PNVP$_{47}$ (LNC P4), OD-PNMVA$_{31}$ (LNC P5), DSPE-PNMVA$_{44}$ (LNC P6), OD-P(NVP$_{27}$coVIm$_{21}$) (LNC P7), DiOD-P(NVP22coVIm15) (LNC P8) and of (B) LNCs post-inserted at 0.5 mM with P7 (LNC P7') or P8 (LNC P8') and LNCs per-formulated at 1 mM with P7 (LNC P7*) or P8 (LNC P8*). Results (n = 3) are expressed as the means ± SD.*

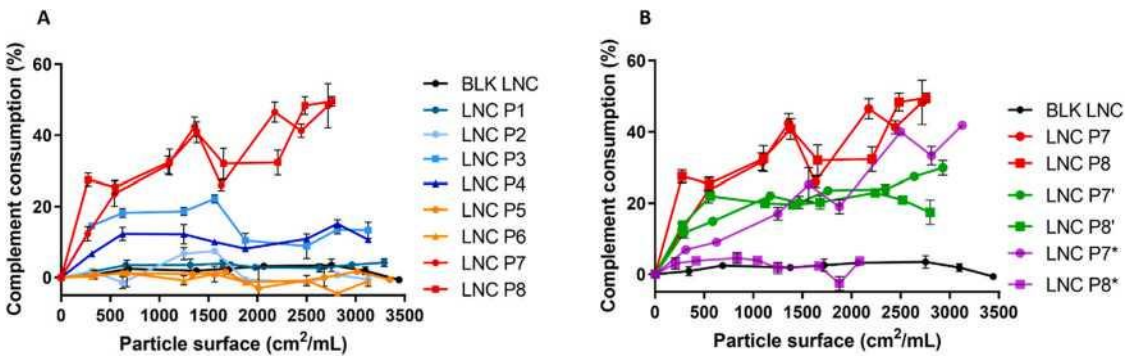

Published in : Colloids and Surfaces B: Biointerfaces (2024), vol. 235, 113788
DOI: 10.1016/j.colsurfb.2024.113788
Status : Postprint (Author's version)

However, even if the density of the polymer at the surface of LNCs certainly influences their stealth properties, it cannot be the only factor for the complement activation difference observed between the per-formulation and the post-modification approach. Indeed, in the case of P7, we clearly see a decrease of the charge surface for the performulation (Fig. 4C compare LNC P7 and LNC P7*) but the latter is not associated to a decrease in the complement activation (Fig. 6B compare LNC P7 and LNC P7*) in contrast to LNC P8 and P8*. Although not well understood at this stage, this behavior was found reproducible, emphasized the key role of the LNCs modifier fine structure and highlighted the great potential of the DiOD-functionalized P8 for LNC modification, in particular via the per-formulation method.

CELL VIABILITY

The impact of the poly(N-vinyl amide) derivatives (P1-P8) and of their corresponding decorated lipid nanocapsules (LNC P1-LNC P8) on cell viability was assessed on B16F10 and HepG2, a murine skin melanoma cell line and a human liver cancer cell line, respectively (Fig. 7).

The cell viability was preserved for both cell lines when exposed to each polymer (P1-P8) at a concentration similar or superior to those used for LNC modification, confirming the intrinsic non-toxicity of these functional NVP-, NMVA- and NVP/VIm-based polymers. Furthermore, the post-modified LNCs (LNC P1-LNC P8) did not show any significant difference in cell viability compared to the blank LNC until 250 µg/mL. At high concentration (1000 µg/mL), the cell viability in presence of the modified LNCs slightly decreased, but apparently in a less extent compared to the blank LNC. The cell viability was not tested for LNCs post-modified at lower polymer concentration (LNC P′) or for the pre-inserted LNCs (LNC P*) but their toxicity is anticipated to be similar or even smaller, given the above demonstrated intrinsic non-toxicity of the polymers at these concentrations.

Published in : Colloids and Surfaces B: Biointerfaces (2024), vol. 235, 113788
DOI: 10.1016/j.colsurfb.2024.113788
Status : Postprint (Author's version)

Fig. 7. *Cell viability of B16F10 and HepG2 cell lines treated with polymers alone and decorated LNCs by these polymers. Cells were incubated with OD-PNVP$_{31}$ (P1), OD-PNVP$_{46}$ (P2), DiOD-PNVP$_{44}$ (P3), DSPE-PNVP$_{47}$ (P4), OD-PNMVA$_{31}$ (P5), DSPE-PNMVA$_{44}$ (P6), OD-P(NVP$_{27}$-co-VIm$_{21}$) (P7) and DiOD-P(NVP$_{22}$-co-VIm$_{15}$) (P8) (concentration range: 0.025–2.5 μM, corresponding to the same dilution than for the LNCs) for 24 h: B16F10 (A), HepG2 (C) to evaluate the impact of the polymers. Cells were also treated with blank LNCs (BLK LNC) and LNCs post-inserted with the different polymers (LNC P1-P8, concentration range: 10–1000 μg/mL) for 24 h: B16F10 (B), HepG2 (D). Cell viability was measured by MTT assay. Results (n = 3) are expressed as the means ± SD.*

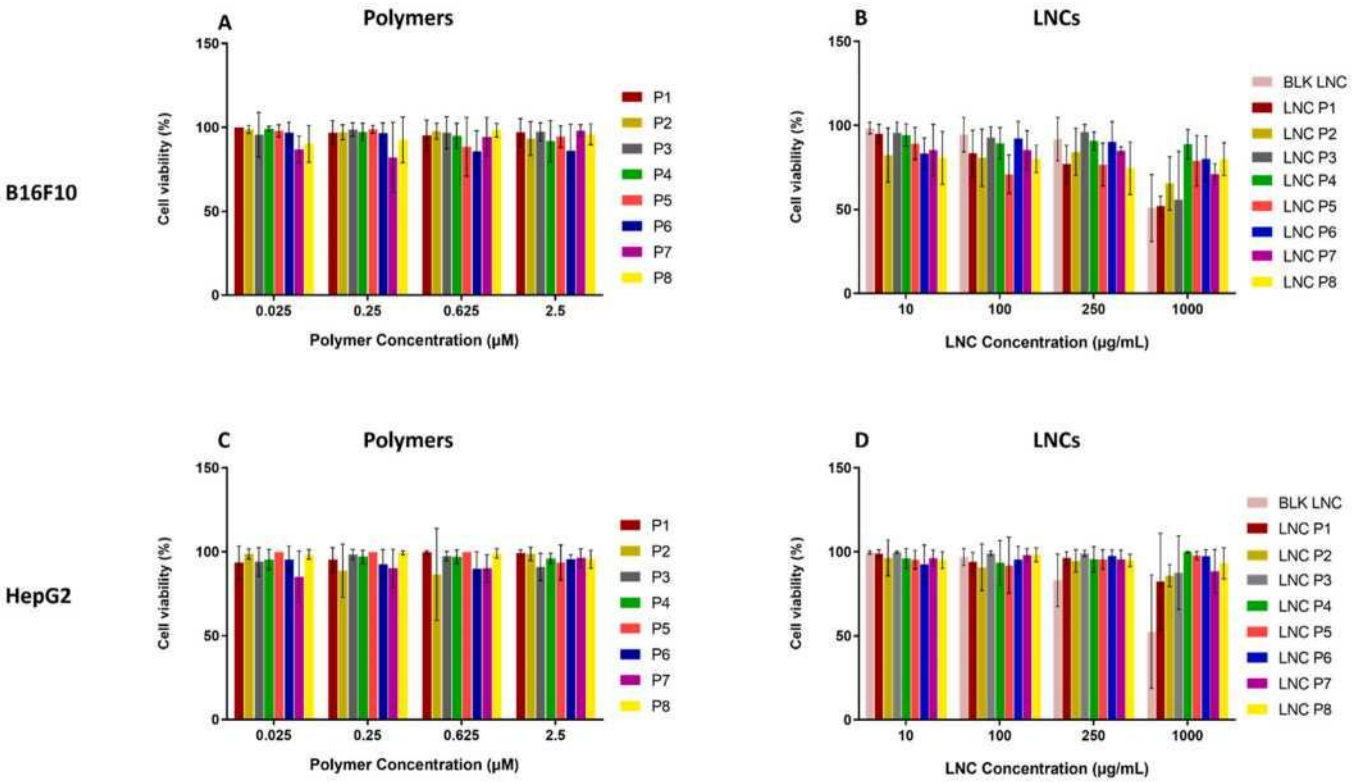

2. Conclusion

The surface modification of drug carriers, including lipid nano-capsules, is a common strategy to prolong their blood residency and to target disease tissues. While pegylation of the nanomedicines remains very popular, the increasing presence of PEG antibodies in the human population and the fact that this approach is restricted to passive targeting constitute strong motivations to develop innovative stealth, responsive and specific PEG alternatives. Here, we described the synthesis of a series of amphiphilic poly(N-vinyl amide) compounds, including pH-responsive ones, and emphasized their potential as LNC modifiers. In addition to OD-PNVP and OD-P(NVP-co-VIm) prepared in previous study [27], was designed a series of novel diversely

Published in : Colloids and Surfaces B: Biointerfaces (2024), vol. 235, 113788
DOI: 10.1016/j.colsurfb.2024.113788
Status : Postprint (Author's version)

substituted compounds associating OD-, DiOD- or DSPE- as hydrophobic chain with PNMVA, PNVP and pH-responsive VIm-containing copolymers. Polymerization were achieved by RAFT in order to guarantee a high level of functionalization and suitable macromolecular characteristic in regards of the application, namely DP around 30–50. The slight preferential incorporation of VIm compared to NVP during radical NVP/VIm copolymerization and the quite homogeneous distribution of the VIm units along the copolymer chains were evidenced by the reactivity ratios determined under RAFT polymerization conditions. This library of polymers was then used for modifying LNC via post-insertion or per-formulation methods at different concentrations. The successful modification of the LNCs was notably assessed by low to moderate increase of the size and dispersity of the carriers compared to the reference samples. Irrespective to the pH, LNC decorated by PNVP or PNMVA associated to OD- and DiOD- remained mostly neutral whereas negatively charged carriers resulted from post-modification of LNC with DSPE-PNVP and DSPE-PNMVA due to the phosphate moiety of DSPE. This characteristic could be exploited in the future in DDS application for the complexation of positively charged active compounds. On the other hand, positive charges appeared at the surface of LNCs modified with the NVP/VIm-based copolymers (functionalized either by OD or DiOD) when pH is decreased below 6.8 due to protonation of the imidazole functions. This pH-responsiveness should allow to target the tumor tissues and facilitate the cellular uptake via cell membrane interactions under acidic tumoral conditions. Contrary to the PNVP- and PNMVA-based LNC modifiers, the VIm-containing copolymers showed buffer effect capacities of interest to enhance the proton sponge effect and promote the endosomal escape. Excellent cell viability was demonstrated for two cell lines for all polymers and their corresponding modified LNCs. Finally, the complement activation level of the modified LNCs evolved in the following order, NVP/VIm > PNVP > PNMVA. In contrast to PNVP, near-zero activation of the complement was observed for the PNMVA decorated LNCs whatever the hydrophobic group, namely OD and DSPE, emphasizing the great potential of this sequence for drug delivery application. Although in an acceptable range, the complement activation rates of the pH-responsive LNCs post-inserted with the VIm-containing copolymers were the highest of the series. However, LNCs pre-inserted with the novel DiOD-P(NVP-co-VIm) showed extremely low complement activation level, which was very promising. This constitutes an important milestone for future studies dedicated to drug encapsulation in these stealth and pH-responsive LNCs, cell internalization and drug release. In summary, this platform synthesis of amphiphilic poly(vinyl amide)-based modifiers offers valuable LNC protective agents from opsonization by complement activation, emphasizes the benefit of using DiOD functionality in the per-formulation method and highlights the interest of PNMVA as PEG alternative.

Published in : Colloids and Surfaces B: Biointerfaces (2024), vol. 235, 113788
DOI: 10.1016/j.colsurfb.2024.113788
Status : Postprint (Author's version)

Moreover, the pH sensitivity of LNCs is an asset with a view to increasing cellular uptake in the acidic tumor microenvironment, opening up new possibilities in the field of active targeting.

CRediT authorship contribution statement

- Lepeletier Elise: Writing - review & editing, Supervision, Methodology, Investigation, Formal analysis, Conceptualization.
- Toussaint François: Writing – original draft, Methodology, Investigation, Formal analysis, Conceptualization
- Pautu Vincent: Methodology, Investigation, Formal analysis.
- Franconi Florence: Methodology, Investigation, Formal analysis.
- Passirani Catherine: Writing - review & editing, Validation, Supervision, Methodology, Investigation, Conceptualization.
- Jerôme Christine: Writing - review & editing, Supervision, Methodology, Investigation, Conceptualization.
- Debuigne Antoine: Writing - review & editing, Writing - original draft, Validation, Supervision, Project administration, Methodology, Investigation, Funding acquisition, Conceptualization.

Declaration of Competing Interest

The authors declare the following financial interests/personal relationships which may be considered as potential competing interests: Antoine Debuigne has patent #EP23171538.4 pending to ULiège. If there are other authors, they declare that they have no known competing financial interests or personal relationships that could have appeared to influence the work reported in this paper.

Data availability

Data will be made available on request.

Acknowledgment

The research was supported by the Wallonia-Brussels Federation (grant for Concerted Research Actions, LIPEGALT project, ULiège), carried out in collaboration with Laboratory of Pharmaceutical Technology and Biopharmacy, CIRM, ULiege (Prof. G. Piel) and the Gene Expression and Cancer Laboratory (GEC), GIGA-Molecular Biology of Diseases, ULiège (Dr. D. Mottet). A.D. is FNRS Senior Research Associate and thanks the F.R.S.-FNRS for financial support.

Published in : Colloids and Surfaces B: Biointerfaces (2024), vol. 235, 113788
DOI: 10.1016/j.colsurfb.2024.113788
Status : Postprint (Author's version)

APPENDIX A. SUPPORTING INFORMATION

Supplementary data associated with this article can be found in the online version at doi:10.1016/j.colsurfb.2024.113788.

Published in : Colloids and Surfaces B: Biointerfaces (2024), vol. 235, 113788
DOI: 10.1016/j.colsurfb.2024.113788
Status : Postprint (Author's version)

References

1. S. Wang, P. Huang, X. Chen, Stimuli-responsive programmed specific targeting in nanomedicine, ACS Nano 10 (2016) 2991–2994, https://doi.org/10.1021/ acsnano.6b00870.
2. S.M. Narum, T. Le, D.P. Le, J.C. Lee, N.D. Donahue, W. Yang, S. Wilhelm, Passive targeting in nanomedicine: fundamental concepts, body interactions, and clinical potential. Nanoparticles Biomed. Appl, Elsevier, 2020, pp. 37–53, https://doi.org/ 10.1016/B978-0-12-816662-8.00004-7.
3. M.S. Bami, M.A. Raeisi Estabragh, P. Khazaeli, M. Ohadi, G. Dehghannoudeh, pH- responsive drug delivery systems as intelligent carriers for targeted drug therapy: brief history, properties, synthesis, mechanism and application, J. Drug Deliv. Sci. Technol. 70 (2022) 102987, https://doi.org/10.1016/j.jddst.2021.102987.
4. N.T. Huynh, C. Passirani, P. Saulnier, J.P. Benoit, Lipid nanocapsules: a new platform for nanomedicine, Int. J. Pharm. 379 (2009) 201–209, https://doi.org/ 10.1016/j.ijpharm.2009.04.026.
5. B. Heurtault, P. Saulnier, B. Pech, J.E. Proust, J.P. Benoit, A novel phase inversion-based process for the preparation of lipid nanocarriers, Pharm. Res. 19 (2002) 875–880, https://doi.org/10.1023/A:1016121319668.
6. E. Garcion, A. Lamprecht, B. Heurtault, A. Paillard, A. Aubert-Pouessel, B. Denizot, P. Menei, J.-P. Benoit, A new generation of anticancer, drug-loaded, colloidal vectors reverses multidrug resistance in glioma and reduces tumor progression in rats, Mol. Cancer Ther. 5 (2006) 1710–1722, https://doi.org/10.1158/1535-7163. MCT-06-0289.

A. Lamprecht, J.-P. Benoit, Etoposide nanocarriers suppress glioma cell growth by intracellular drug delivery and simultaneous P-glycoprotein inhibition, J. Control. Release 112 (2006) 208–213, https://doi.org/10.1016/j.jconrel.2006.02.014.

7. G.-E. Fathy Abd-Ellatef, E. Gazzano, D. Chirio, A. Ragab Hamed, D.C. Belisario, C. Zuddas, E. Peira, B. Rolando, J. Kopecka, M. Assem Said Marie, S. Sapino, S. Ramadan Fahmy, M. Gallarate, A.-H. Zaki Abdel-Hamid, C. Riganti, Curcumin- loaded solid lipid nanoparticles bypass P-glycoprotein mediated doxorubicin resistance in triple negative breast cancer cells, Pharmaceutics 12 (2020) 96, https://doi.org/10.3390/pharmaceutics12020096.
8. E. Allard, C. Passirani, E. Garcion, P. Pigeon, A. Vessières, G. Jaouen, J.-P. Benoit, Lipid nanocapsules loaded with an organometallic tamoxifen derivative as a novel drug-carrier system for experimental malignant gliomas, J. Control. Release 130 (2008) 146–153, https://doi.org/10.1016/j.jconrel.2008.05.027.
9. E. Allard, N.T. Huynh, A. Vessières, P. Pigeon, G. Jaouen, J.-P. Benoit, C. Passirani, Dose effect activity of ferrocifen-loaded lipid nanocapsules on a 9L-glioma model, Int. J. Pharm. 379 (2009) 317–323, https://doi.org/10.1016/j.ijpharm.2009.05.031.

Published in : Colloids and Surfaces B: Biointerfaces (2024), vol. 235, 113788
DOI: 10.1016/j.colsurfb.2024.113788
Status : Postprint (Author's version)

10. E. Allard, D. Jarnet, A. Vessières, S. Vinchon-Petit, G. Jaouen, J.-P. Benoit, C. Passirani, Local delivery of ferrociphenol lipid nanocapsules followed by external radiotherapy as a synergistic treatment against intracranial 9L glioma xenograft, Pharm. Res. 27 (2010) 56–64, https://doi.org/10.1007/s11095-009- 0006-0.
11. N.T. Huynh, M. Morille, J. Bejaud, P. Legras, A. Vessières, G. Jaouen, J.-P. Benoit, C. Passirani, Treatment of 9L gliosarcoma in rats by ferrociphenol-loaded lipid nanocapsules based on a passive targeting strategy via the EPR effect, Pharm. Res. 28 (2011) 3189–3198, https://doi.org/10.1007/s11095-011-0501-y.
12. A.-L. Laine, N.T. Huynh, A. Clavreul, J. Balzeau, J. Béjaud, A. Vessières, J.- P. Benoit, J. Eyer, C. Passirani, Brain tumour targeting strategies via coated ferrociphenol lipid nanocapsules, Eur. J. Pharm. Biopharm. 81 (2012) 690–693, https://doi.org/10.1016/j.ejpb.2012.04.012.
13. N.T. Huynh, C. Passirani, E. Allard-Vannier, L. Lemaire, J. Roux, E. Garcion, A. Vessières, J.-P. Benoit, Administration-dependent efficacy of ferrociphenol lipid nanocapsules for the treatment of intracranial 9L rat gliosarcoma, Int. J. Pharm. 423 (2012) 55–62, https://doi.org/10.1016/j.ijpharm.2011.04.037.
14. A.-L. Laine, E. Adriaenssens, A. Vessières, G. Jaouen, C. Corbet, E. Desruelles, P. Pigeon, R.-A. Toillon, C. Passirani, The in vivo performance of ferrocenyl tamoxifen lipid nanocapsules in xenografted triple negative breast cancer, Biomaterials 34 (2013) 6949–6956, https://doi.org/10.1016/j.biomaterials.2013.05.065.
15. A.-L. Laine, A. Clavreul, A. Rousseau, C. Tetaud, A. Vessieèes, E. Garcion,
16. G. Jaouen, L. Aubert, M. Guilbert, J.-P. Benoit, R.-A. Toillon, C. Passirani, Inhibition of ectopic glioma tumor growth by a potent ferrocenyl drug loaded into stealth lipid nanocapsules, Nanomed. Nanotechnol. Biol. Med. 10 (2014) 1667–1677, https://doi.org/10.1016/j.nano.2014.05.002.
17. S. Topin-Ruiz, A. Mellinger, E. Lepeltier, C. Bourreau, J. Fouillet, J. Riou, G. Jaouen, L. Martin, C. Passirani, N. Clere, p722 ferrocifen loaded lipid nanocapsules improve survival of murine xenografted-melanoma via a potentiation of apoptosis and an activation of CD8+ T lymphocytes, Int. J. Pharm. 593 (2021) 120111, https://doi.org/10.1016/j.ijpharm.2020.120111.
18. T. Perrier, P. Saulnier, F. Fouchet, N. Lautram, J.-P. Benoît, Post-insertion into Lipid NanoCapsules (LNCs): From experimental aspects to mechanisms, Int. J. Pharm. 396 (2010) 204–209, https://doi.org/10.1016/j.ijpharm.2010.06.019.
19. A.-L. Laine, J. Gravier, M. Henry, L. Sancey, J. Béjaud, E. Pancani, M. Wiber,Texier, J.-L. Coll, J.-P. Benoit, C. Passirani, Conventional versus stealth lipid nanoparticles: formulation and in vivo fate prediction through FRET monitoring, J. Control. Release 188 (2014) 1–8, https://doi.org/10.1016/j.jconrel.2014.05.042.

Published in : Colloids and Surfaces B: Biointerfaces (2024), vol. 235, 113788
DOI: 10.1016/j.colsurfb.2024.113788
Status : Postprint (Author's version)

20. B. Heurtault, P. Saulnier, B. Pech, J. Proust, J. Benoît, Properties of polyethylene glycol 660 12-hydroxy stearate at a triglyceride/water interface, Int. J. Pharm. 242 (2002) 167–170, https://doi.org/10.1016/S0378-5173(02)00144-8.

21. G.T. Kozma, T. Shimizu, T. Ishida, J. Szebeni, Anti-PEG antibodies: properties, formation, testing and role in adverse immune reactions to PEGylated nano-biopharmaceuticals, Adv. Drug Deliv. Rev. 154–155 (2020) 163–175, https://doi. org/10.1016/j.addr.2020.07.024.

22. S. Zalba, T.L.M. ten Hagen, C. Burgui, M.J. Garrido, Stealth nanoparticles in oncology: facing the PEG dilemma, J. Control. Release 351 (2022) 22–36, https:// doi.org/10.1016/j.jconrel.2022.09.002.

23. M. Ibrahim, E. Ramadan, N.E. Elsadek, S.E. Emam, T. Shimizu, H. Ando, Y. Ishima, O.H. Elgarhy, H.A. Sarhan, A.K. Hussein, T. Ishida, Polyethylene glycol (PEG): the nature, immunogenicity, and role in the hypersensitivity of PEGylated products, J. Control. Release 351 (2022) 215–230, https://doi.org/10.1016/j.jconrel.2022.09.031.

24. S. Hirsjärvi, S. Dufort, G. Bastiat, P. Saulnier, C. Passirani, J.L. Coll, J.P. Benoît, Surface modification of lipid nanocapsules with polysaccharides: from physicochemical characteristics to in vivo aspects, Acta Biomater. 9 (2013) 6686–6693, https://doi.org/10.1016/j.actbio.2013.01.038.

25. A. Beduneau, P. Saulnier, F. Hindre, A. Clavreul, J.-C. Leroux, J.-P. Benoit, Design of targeted lipid nanocapsules by conjugation of whole antibodies and antibody Fab' fragments, Biomaterials 28 (2007) 4978–4990, https://doi.org/10.1016/j. biomaterials.2007.05.014.

26. R. Karim, E. Lepeltier, L. Esnault, P. Pigeon, L. Lemaire, C. Lépinoux-Chambaud, N. Clere, G. Jaouen, J. Eyer, G. Piel, C. Passirani, Enhanced and preferential internalization of lipid nanocapsules into human glioblastoma cells: effect of a surface-functionalizing NFL peptide, Nanoscale 10 (2018) 13485–13501, https:// doi.org/10.1039/C8NR02132E.

27. V. Pautu, E. Lepeltier, A. Mellinger, J. Riou, A. Debuigne, C. Jerome, N. Clere, C. Passirani, pH-Responsive lipid nanocapsules: a promising strategy for improved resistant melanoma cell internalization, Cancers 13 (2021) 2028, https://doi.org/ 10.3390/cancers13092028 CO - CANCCT.

28. M. Berger, F. Toussaint, S.Ben Djemaa, J. Laloy, H. Pendeville, B. Evrard, C. Jerome, A. Lechanteur, D. Mottet, A. Debuigne, G. Piel, Poly(vinyl pyrrolidone) derivatives as PEG alternatives for stealth, non-toxic and less immunogenic siRNA-containing lipoplex delivery, J. Control. Release 361 (2023) 87–101, https://doi. org/10.1016/j.jconrel.2023.07.031.

29. M. Berger, F. Toussaint, S. Ben Djemaa, E. Maquoi, H. Pendeville, B. Evrard, C. Jerome, J. Leblond Chain, A. Lechanteur, D. Mottet, A. Debuigne, G. Piel, Poly(N -methyl- N -vinylacetamide): a strong alternative to PEG for lipid-based nanocarriers delivering siRNA, Adv. Healthc. Mater. (2023) 2302712, https://doi. org/10.1002/adhm.202302712.

30. S.Z. Zard, Discovery of the RAFT/MADIX process: mechanistic insights and polymer chemistry implications, Macromolecules 53 (2020) 8144–8159, https:// doi.org/10.1021/acs.macromol.0c01441.

Published in : Colloids and Surfaces B: Biointerfaces (2024), vol. 235, 113788
DOI: 10.1016/j.colsurfb.2024.113788
Status : Postprint (Author's version)

31. S. Perrier, 50th Anniversary perspective: RAFT polymerization - a user guide, Macromolecules 50 (2017) 7433–7447, https://doi.org/10.1021/acs.macromol.7b00767.
32. M.R. Hill, R.N. Carmean, B.S. Sumerlin, Expanding the scope of RAFT polymerization: recent advances and new horizons, Macromolecules 48 (2015) 5459–5469, https://doi.org/10.1021/acs.macromol.5b00342.
33. B.Tilottama, K. Manojkumar, P.M. Haribabu, K. Vijayakrishna, A short review on RAFT polymerization of less activated monomers, J. Macromol. Sci. Part A Pure Appl. Chem. 59 (2022) 180–201, https://doi.org/10.1080/ 10601325.2021.2024076.
34. S. Harrisson, X. Liu, J.N. Ollagnier, O. Coutelier, J.D. Marty, M. Destarac, RAFT polymerization of vinyl esters: Synthesis and applications, Polymers (Basel) 6 (2014) 1437–1488, https://doi.org/10.3390/polym6051437.
35. N. Roka, O. Kokkorogianni, P. Kontoes-Georgoudakis, I. Choinopoulos, M. Pitsikalis, Recent advances in the synthesis of complex macromolecular architectures based on poly(N-vinyl pyrrolidone) and the RAFT polymerization technique, Polym. (Basel) 14 (2022) 701, https://doi.org/10.3390/ polym14040701.
36. L. McDowall, G. Chen, M.H. Stenzel, Synthesis of seven-arm poly(vinyl pyrrolidone) star polymers with lysozyme core prepared by MADIX/RAFT polymerization, Macromol. Rapid Commun. 29 (2008) 1666–1671, https://doi. org/10.1002/marc.200800416.
37. M. Langlais, O. Coutelier, M. Destarac, Thiolactone-functional reversible deactivation radical polymerization agents for advanced macromolecular engineering, Macromolecules 51 (2018) 4315–4324, https://doi.org/10.1021/acs. macromol.8b00770.
38. G. Pound, J.M. McKenzie, R.F.M. Lange, B. Klumperman, Polymer-protein conjugates from ω-aldehyde endfunctional poly(N-vinylpyrrolidone) synthesised via xanthate-mediated living radical polymerisation, Chem. Commun. (2008) 3193–3195, https://doi.org/10.1039/b803952f.
39. A.Dupre-Demorsy, O. Coutelier, M. Destarac, C. Nadal, V. Bourdon, T. Ando, H. Ajiro, RAFT polymerization of N-methyl-N-vinylacetamide and related double hydrophilic block copolymers, Macromolecules 55 (2022) 1127–1138, https://doi. org/10.1021/acs.macromol.1c01593.
40. N.T. Huynh, C. Passirani, P. Saulnier, J.P. Benoit, Lipid nanocapsules: a new platform for nanomedicine, Int. J. Pharm. 379 (2009) 201–209, https://doi.org/ 10.1016/j.ijpharm.2009.04.026.
41. B. Heurtault, P. Saulnier, J.-P. Benoit, J.-E. Proust, B. Pechn, J. Richard, Lipid Nanocapsules, methods of preparation and use as a medicament., FR2805761B1, 2022.
42. Z. Zhong, J. Feijen, M.C. Lok, W.E. Hennink, L.V. Christensen, J.W. Yockman, Y.- H. Kim, S.W. Kim, Low molecular weight linear polyethylenimine- b -poly(ethylene glycol)- b -polyethylenimine triblock copolymers: synthesis, characterization, and in vitro gene transfer properties, Biomacromolecules 6 (2005) 3440–3448, https:// doi.org/10.1021/bm050505n.

Published in : Colloids and Surfaces B: Biointerfaces (2024), vol. 235, 113788
DOI: 10.1016/j.colsurfb.2024.113788
Status : Postprint (Author's version)

43. B. Passirani, G. Barratt, J.-P. Devissaguet, D. Labarre, Interactions of nanoparticles bearing heparin or dextran covalently bound to poly(methyl methacrylate) with the complement system, Life Sci. 62 (1998) 775–785, https://doi.org/10.1016/ S0024-3205(97)01175-2.

44. Z. Ge, D. Xie, D. Chen, X. Jiang, Y. Zhang, H. Liu, S. Liu, Stimuli-responsive double hydrophilic block copolymer micelles with switchable catalytic activity, Macromolecules 40 (2007) 3538–3546, https://doi.org/10.1021/ma070550i.

45. C. Peng, K. Huang, M. Han, W. Meng, Y. Xiong, W. Xu, Facile synthesis and catalytic activity of well-defined amphiphilic block copolymers based on N -vinylimidazolium, Polym. Adv. Technol. 24 (2013) 1089–1093, https://doi.org/ 10.1002/pat.3193.

46. A.Wamsley, B. Jasti, P. Phiasivongsa, X. Li, Synthesis of random terpolymers and determination of reactivity ratios ofN-carboxyanhydrides of leucine, ?-benzyl aspartate, and valine, J. Polym. Sci. Part A Polym. Chem. 42 (2004) 317–325, https://doi.org/10.1002/pola.11020.

47. J.M. Ting, T.S. Navale, F.S. Bates, T.M. Reineke, Precise compositional control and systematic preparation of multimonomeric statistical copolymers, ACS Macro Lett. 2 (2013) 770–774, https://doi.org/10.1021/mz4003112.

48. M. Fineman, S.D. Ross, Linear method for determining monomer reactivity ratios in copolymerization, J. Polym. Sci. 5 (1950) 259–262, https://doi.org/10.1002/ pol.1950.120050210.

49. T. Kelen, F. Tudos, Analysis of the linear methods for determining copolymerization reactivity ratios. I. A new improved linear graphic method, J. Macromol. Sci. Part A - Chem. 9 (1975) 1–27, https://doi.org/10.1080/ 00222337508068644.

50. A. Vonarbourg, P. Saulnier, C. Passirani, J.P. Benoit, Electrokinetic properties of noncharged lipid nanocapsules: Influence of the dipolar distribution at the interface, Electrophoresis 26 (2005) 2066–2075, https://doi.org/10.1002/ elps.200410145.

51. T. Hakamatani, S. Asayama, H. Kawakami, Synthesis of alkylated poly(1- vinylimidazole) for a new pH-sensitive DNA carrier, Nucleic Acids Symp. Ser. 52 (2008) 677–678, https://doi.org/10.1093/nass/nrn342.

52. C.R.T. Tarley, M.Z. Corazza, B.F. Somera, M.G. Segatelli, Preparation of new ion- selective cross-linked poly(vinylimidazole-co-ethylene glycol dimethacrylate) using a double-imprinting process for the preconcentration of Pb2+ ions, J. Colloid Interface Sci. 450 (2015) 254–263, https://doi.org/10.1016/j.jcis.2015.02.074.

53. G. Liu, Y. Li, V.R. Sheth, M.D. Pagel, Imaging in vivo extracellular pH with a single paramagnetic chemical exchange saturation transfer magnetic resonance imaging contrast agent, Mol. Imaging 11 (2012) 47-57. (http://www.ncbi.nlm.nih.gov/ pubmed/22418027).

54. O. Boussif, F. Lezoualc'h, M.A. Zanta, M.D. Mergny, D. Scherman, B. Demeneix, J. P. Behr, A versatile vector for gene and oligonucleotide transfer into cells in culture and in vivo: polyethylenimine, Proc. Natl. Acad. Sci. 92 (1995) 7297–7301, https://doi.org/10.1073/pnas.92.16.7297.

Published in : Colloids and Surfaces B: Biointerfaces (2024), vol. 235, 113788
DOI: 10.1016/j.colsurfb.2024.113788
Status : Postprint (Author's version)

55. S. Asayama, S. Nishinohara, H. Kawakami, Zinc-chelated poly(1-vinylimidazole) and a carbohydrate ligand polycation form DNA ternary complexes for gene delivery, Bioconjug. Chem. 22 (2011) 1864–1868, https://doi.org/10.1021/ bc2003378.

56. A. Vonarbourg, C. Passirani, P. Saulnier, P. Simard, J.C. Leroux, J.P. Benoit, Evaluation of pegylated lipid nanocapsules versus complement system activation and macrophage uptake, J. Biomed. Mater. Res. Part A. 78A (2006) 620–628, https://doi.org/10.1002/jbm.a.30711.